
Check for updates

LEIS is an extremely surface sensitive method to analyse the elemental composition of the first monolayers of a sample [7]. In LEIS, a beam of low energy (few keV) singly charged ions (usually noble gas ions) is directed toward the surface and ions scattered under a certain angle pass an energy analyser and are detected and counted [8]. The collision process can be described in binary collision approximation which allows straightforward to infer the mass of the atom from which the detected projectile atom has been scattered [9].

The used LEIS apparatus is described in detail in [10]. In brief, ions are produced in a Bayard-Alpert type ion source, extracted from the source volume with a voltage of about 100 V, and accelerated by a second electrode to their final energy of $q \times 1$ kV, where q denotes the charge of the ion. A 90° magnetic sector field is used to select the mass and charge state of the probing ion beam. Two sets of ion optical elements, each one consisting of an einzel lens and steering plates for lateral and vertical beam deflection, are mounted before and after the magnetic sector field and guide and focus the ion beam onto the sample. The sample is mounted on a Prevac PTS 1000 RES/C-K sample holder which can be resistively heated up to 1200 K and allows to measure the temperature of the front plate with a K-type thermocouple. The scattered ions pass a 90° spherical energy analyser and are counted with a channeltron electron multiplier. The sample holder and the analyser can be independently turned around the scattering centre in order to adjust incident angle and scattering angle of the ions. The setting and scanning of the voltages at the analyser electrodes as well as the ion counting is performed with a National Instruments PXI-8106 data acquisition board which is controlled by a personal computer running LabVIEW software. Sample cleaning and sputter erosion is done with a Perkin–Elmer 04–161 sputter ion gun.

The WCrY alloy is produced by a field-assisted sintering technology [5]. The composition of the produced WCrY alloy is given in Table 1. The WCrY ingot obtained after sintering is first cut by wire erosion to get a sample which measures 10 mm x 5 mm x 1 mm. The sample is manually ground to remove residual impurities from cutting. For grinding silicon-carbide (SiC) papers with different particle sizes are used. Afterwards a cloth with a diamond paste of particle size 1 μm is applied. Finally, the sample is polished to a mirror finish using an Active Oxide Polishing Suspension (OPS) with 0.04 μm SiO_2 particles.

Prior to the LEIS measurements the sample is in-situ cleaned by sputtering with 500 eV Kr^+ ions under normal incidence with a total fluence in the order of $1 \times 10^{21} m^{-2}$. It is almost unavoidable that the cleaning procedure by sputtering will already modify the surface because the sputtering yields for the various constituents of the WCrY sample are different. As a result the surface concentrations of the cleaned sample deviate from the bulk concentrations. The deviation of the surface concentrations from the respective bulk concentrations can be derived from the equilibrium state which depends on the sputter yields and is for a two component alloy given by [11]

$$\frac{c_{s,1}}{c_{s,2}} = \frac{Y_2}{Y_1}\frac{c_{b,1}}{c_{b,2}}, \tag{1}$$

where c denotes the surface/bulk concentration and Y is the sputter yield. Indices s and b refer to surface and bulk, respectively, and numbers label the alloy constituents. Kr is deliberately chosen as sputter gas because the sputter yields for W and Cr at the low ion energy of 500 eV do not differ very much. The elemental sputtering yields of

Table 1
Bulk composition of the WCrY alloy sample.

	W	Cr	Y
weight%	88.0	11.4	0.6
atom%	67.9	31.1	1.0

500 eV Kr^+ ions for pure
Since the difference in sputtering y
resultant deviation in surface densities is
it is anticipated that surface changes due to thermal
preferential sputtering by low energy deuterons will be much larger
can easily be distinguished from the artefacts of surface cleaning.

The mass resolution of LEIS depends on the mass ratio between the probing ion and the surface atoms [13]. In that respect it would be beneficial to use incident ions with a higher mass, e.g. Ne^+ or Ar^+. However, due to the larger masses of these ions they would induce stronger sputtering of the surface which might lead to unintended changes of the surface composition. He^+ is chosen as probing ion in order to keep those effects reasonably small. Although the mass resolution is not optimum, the amplitudes of the various peaks in the scattering spectra can be well determined by the peak fitting procedure outlined below. For the LEIS measurements of the thermally activated Cr (and Y) segregation, the energy spectra of 1 keV He^+ ions are measured at various sample temperatures between room temperature (RT) and 1000 K. The ion beam hits the sample surface under an angle of 20° with respect to the surface normal and reflected ions are detected at a scattering angle of $\theta = 140°$.

The investigation of the W enrichment by preferential sputtering is performed using a D_2^+ ion beam with an energy of 500 eV, i.e. 250 eV per deuteron. The ions are produced by electron impact on D_2. According to [14] most ionisation events result in molecular D_2^+ ions[1], but up to 7% of the ionising collisions lead to dissociation and produce D^+ ions which hit the sample at an energy of 500 eV. Deuteron fluxes of the order of $1 \times 10^{18} m^{-2}s^{-1}$ are supplied by the sputter ion gun and, after integration for few hours, applied fluences amount to several $10^{21} m^{-2}$. Since the used D_2 gas has 99.8% purity and the sputter ion gun has no mass selection, the gas is fed via a LN_2 cold trap in order to freeze out any contaminants. The elemental sputtering yield of 250 eV deuterons for Cr is about 0.04 and the yield for W is less than 3×10^{-4}, i.e. lower by at least a factor of 100 [15]. The difference in sputter yields for the small fraction of D^+ ions with 500 eV in the beam is still a factor of 30 to 40 but will have only weak influence on the effect of preferential sputtering. The LEIS measurements are taken again with He^+ ions at an impact energy of 1 keV under a scattering angle of 140°.

An example of a recorded LEIS spectrum is shown in Fig. 1. The spectrum shows the energy distribution of the He^+ ions scattered from the WCrY sample surface while it is heated to a temperature of 800 K. The measuring time for this spectrum is about 15 min. The largest peak at the right part of the spectrum results from scattering from W atoms ($E = 930$ eV), two smaller peaks due to scattering from Y ($E = 855$ eV) and Cr ($E = 760$ eV) atoms are embedded in the pronounced left wing of the W peak. This wing results from quite strong re-ionisation of He projectiles undergoing multiple scattering events on atoms in deeper layers and therefore losing more energy. The small peak at $E = 400$ eV indicates scattering from O atoms on the surface originating mainly from the yttria which is contained in the alloyed powder before sintering [16]. Another source could be the adsorption of O_2 from the residual gas, although the base pressure in the apparatus is below 5×10^{-8} Pa, limiting the oxygen exposure to less than 0.3 Lh^{-1}. The various peaks in the spectra are fitted with Gaussians (dashed and dotted lines) and the inelastic re-ionisation background is fitted with a modified formula[2] originally proposed in [17] (grey line). The sum of all fitted contributions (black line) shows good agreement with the

[1] The ion source is operated at a gas pressure of $\approx 1 \times 10^{-2}$Pa which gives a Knudsen number $K_n \gg 1$. At these large free paths for electrons and ions the number of generated D_3^+ ions is negligible.

[2] The modifications are (i) the introduction of another parameter adjusting the slope of the background at the peak position and (ii) the limitation of the exponentially rising term which is kept constant for energies above the peak energy. These modifications result in considerably lower residues.

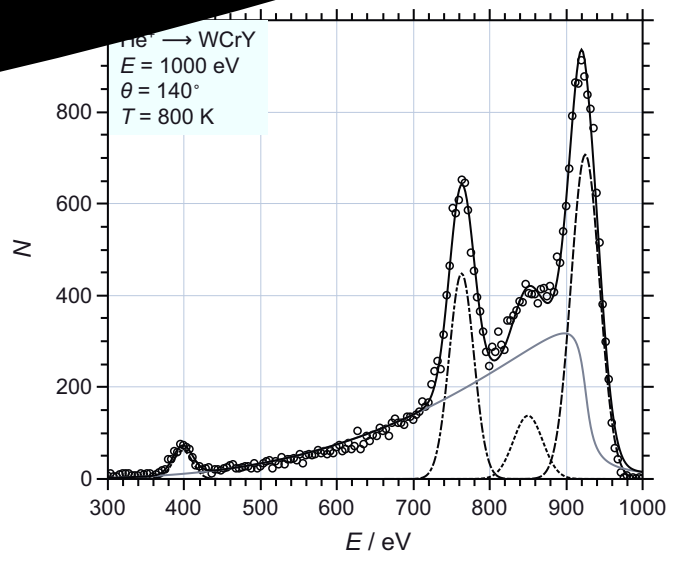

Fig. 1. LEIS spectrum measured at a sample temperature of 800 K. The number of counts, N, is plotted versus the energy, E, of the respective channel. Measured data points are drawn with open circles, the peaks in the spectrum are fitted with Gaussians: Cr (dashed-dotted line), Y(dotted line), W(dashed line). The re-ionisation background from W is plotted with the grey line. The small peak at 400 eV originates from O. The sum of all contributions is given by the full black line.

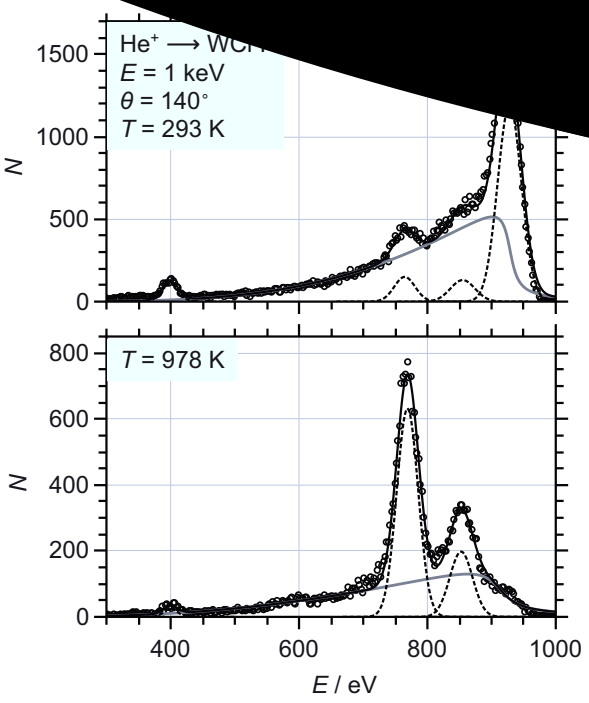

Fig. 2. Two LEIS spectra measured at RT (top) and at $T = 978$ K (bottom). In both spectra the Gaussian peak fits for W, Y, Cr, and O are shown with dotted black lines. The re-ionisation underground is given by the full grey line and the sum of all contributions is plotted with the full black line.

measured spectrum.

The magnitude A_i of an individual peak originating from scattering at atoms of species i is given as the area under the fitted peak which is proportional to the product of peak amplitude and full width of half maximum, both obtained from the peak fitting procedure. The uncalibrated surface concentration c_i for species i on the surface is defined as

$$c_i = \frac{A_i}{\sum_j A_j} \tag{2}$$

where the summation goes over all elements j on the surface. The magnitude of an individual peak depends on the differential scattering cross section multiplied with the probability that the projectile ion is not neutralised during the collision. This quantity might be obtained from calibration measurements using pure elemental samples of the various alloy species. Unfortunately, such measurements are not yet available. However, since $c_i(A_1, ., A_n)$ defined in Eq. (2) is asymptotically correct for zero ($c = 0$) and full ($c = 1$) coverage, and strictly monotonous in between, it fulfils the requirements to characterise the surface coverage.

3. Results and discussion

Two representative LEIS spectra for the investigation of the thermally activated segregation of Cr and Y are shown in Fig. 2. The spectrum at the top is measured at RT after cleaning the sample with 500 eV Kr^+ sputtering. The peak fitting procedure yields four distinct peaks originating from O, Cr, Y, and W (from left to right). The spectrum shows a pronounced re-ionisation background. The sum of the four Gaussians and the background show a good agreement with the measured data.

The LEIS spectrum at the bottom is measured at a sample temperature of 978 K. The Cr ($E = 760$ eV) and Y ($E = 855$ eV) peaks are much larger compared to the measurement at RT, indicating that segregation to the surface of both constituents has occurred. Again, the fitting procedure yields reasonably good agreement with the measurement. However, the W peak at $E = 930$ eV is suppressed, suggesting that there are almost no W atoms remaining in the top surface layer. There is nevertheless an inelastic background contribution, extending to the original W peak position. This shows that W atoms are still present in deeper layers and He atoms (multiply) scattered at deeper layers are re-ionised when leaving the sample.

The measurements of the surface concentrations are performed several times. Each run is started with sufficient sputter cleaning of the sample, thus removing the top surface layers until the LEIS spectra look similar to the spectrum shown in Fig. 2 at the top. Following the cleaning step the sample is heated in increasing steps up to a maximum of 1000 K. LEIS spectra are recorded for each temperature step and the surface concentrations of O, Cr, Y, and W are determined. Fig. 3 depicts a compilation of all acquired data. The surface concentrations change little for temperatures up to about 600 K. Increasing the temperature further leads to strong increases of the Cr and Y concentrations and a corresponding decrease of the W surface density. The strong segregation occurs in the temperature range 720 K to 860 K. As already seen at the bottom of Fig. 2, no W atoms in the top surface layer are detected by LEIS at a temperature of 1000 K.

The segregation enthalpy, ΔH, can be determined from the data shown in Fig. 3. For the analysis of the Cr segregation we follow the procedure described in [18]. The surface concentration of the segregating species, here Cr, is described by a Langmuir-McLean relation [19]

$$\frac{c^s_{Cr}}{1 - c^s_{Cr}} = \frac{c^b_{Cr}}{1 - c^b_{Cr}} \exp\left(\frac{-\Delta G}{kT}\right), \tag{3}$$

where c^s_{Cr} denotes the fractional surface coverage of Cr, c^b_{Cr} the fractional Cr bulk concentration, and ΔG is the Gibbs free energy of segregation. Using $\Delta G = \Delta H - T\Delta S$, where S is the entropy, and taking the logarithm of Eq. 3 gives the following equation [20]

$$\ln\left(\frac{c^s_{Cr}}{1 - c^s_{Cr}}\right) = \frac{-\Delta H}{k} \times \frac{1}{T} + const. \tag{4}$$

Fig. 4 shows the corresponding Arrhenius plot of the Cr surface concentration data. The data points are clearly separated in two distinct regions. At temperatures below 700 K (right part of the figure) the Cr

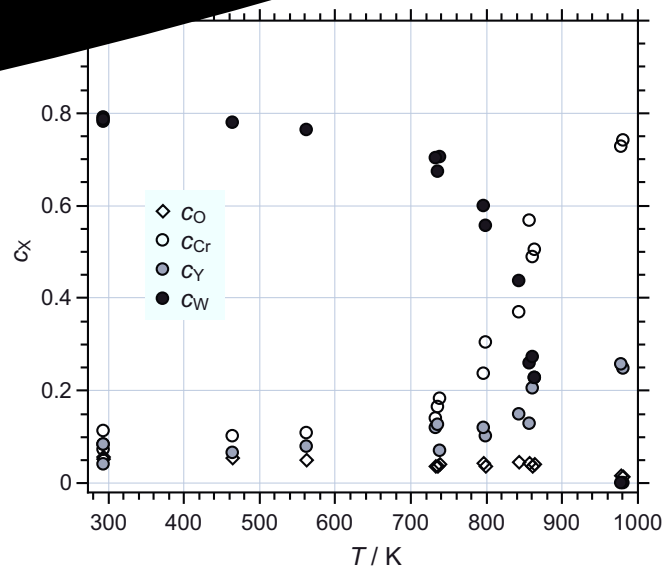

Fig. 3. The fractional surface concentrations, c_X, determined from the fitted peaks in the LEIS spectra according to Eq. (2) for O, Cr, Y, and W are plotted versus the sample temperature, T.

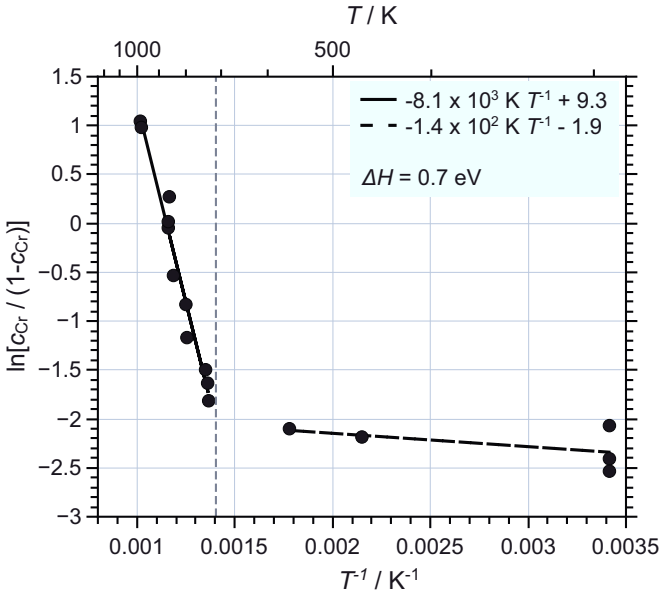

Fig. 4. Arrhenius plot of the Langmuir-McLean relation (Eq. (3)) for Cr with straight line fits for the high temperature (above 700 K) and low temperature regions. The logarithm of the surface coverage, $\ln(\frac{c^S_{Cr}}{1-c^S_{Cr}})$, is plotted versus the reciprocal temperature, T^{-1}. A temperature scale is drawn on top of the figure.

surface concentration changes little with increasing temperature, whereas at higher temperatures a strong increase of Cr surface coverage with increasing temperature is visible. The lines in the figure are linear regression curves according to Eq. (4) where the data above and below 700 K are fitted separately. The segregation enthalpy in the high temperature region determined from the slope of the linear regression line is $\Delta H = 0.7\,\text{eV}$. Both lines cross at a critical temperature of $T_{c,Cr} = 712\,\text{K}$.

For the low temperature region we refrain from evaluation of a segregation enthalpy because it is not clear that the slight increase of Cr surface concentrations with rising temperature is indeed a thermal

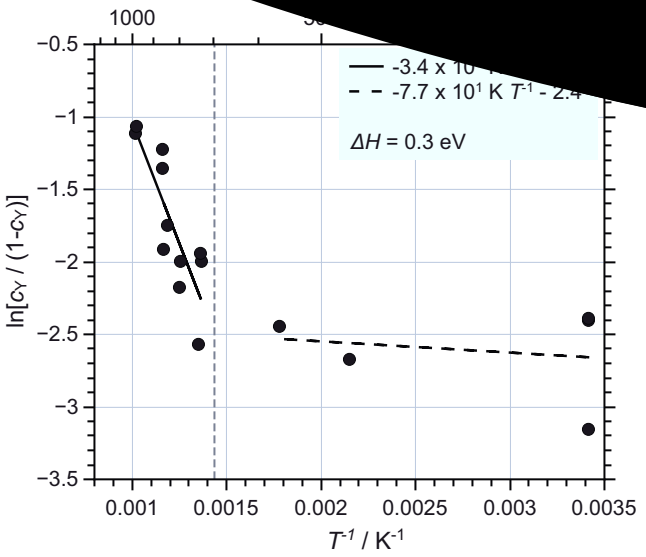

Fig. 5. Arrhenius plot of the Langmuir-McLean relation (Eq. (3)) for Y with straight line fits for the high temperature (above 700 K) and low temperature regions. The logarithm of the surface coverage, $\ln(\frac{c^S_Y}{1-c^S_Y})$, is plotted versus the reciprocal temperature, T^{-1}.

segregation as in the high temperature region. As mentioned in the experimental section, the sputter cleaning with Kr^+ causes some preferential erosion which leads according to Eq. (1) to a surface depletion of the species with the larger sputter yield, which is Cr. The small increase when raising the sample temperature to 600 K to 700 K, which is less than a factor of 2, is likely due to recovery of the unperturbed surface densities due to Cr diffusion from the bulk.

The same analysis for the Y surface concentration is shown in Fig. 5. Again, the data is separated in two regions with slow and fast segregation, respectively. The segregation enthalpy for Y is $\Delta H = 0.3\,\text{eV}$. The critical temperature where both straight lines cross is $T_{c,Y} = 696\,\text{K}$. This temperature is not significantly different from the critical temperature obtained for Cr segregation.

It is obvious that for both lighter alloy constituents, Cr and Y, the segregation behaviour looks very similar. In both cases segregation proceeds rather slowly below a critical temperature and accelerates as soon as this temperature is exceeded. However, it is not clear what happens at the transition temperature. Unfortunately, a ternary phase diagram of WCrY is not available in the literature. Looking at the binary phase diagram of W-Cr, such as e.g. published in [21], the point of interest, $T = 700\,\text{K}$ at a Cr content of 31%, is located in the miscibility gap far from any phase boundary. Here, the W-Cr alloy consists of a mixture of two phases called α_1 and α_2 which are Cr-rich and W-rich solute solutions. The observed Cr surface enrichment might be attributed to grain boundary segregation of these phases.

After having quantified the segregation behaviour, an interesting questions arises: What happens with the Cr/Y layer at the grain boundaries when the sample cools down? This can be investigated with LEIS, too, but some attention has to be paid to the unavoidable sputtering by the He^+ ions used for the analysis. Sputtering by the probing ion beam is of no concern for the previous analysis of the thermally driven segregation behaviour, but here it needs to be discriminated against a possible de-segregation. In order to keep the (preferential) sputtering and thus the surface modification during the measurements as low as possible, the experiment is conducted in the following way: The sample is cleaned by Kr sputtering and heated to the desired temperature of 1000 K. It is kept at this temperature for sufficient time (about 1h) to allow the segregation to reach an equilibrium. The time

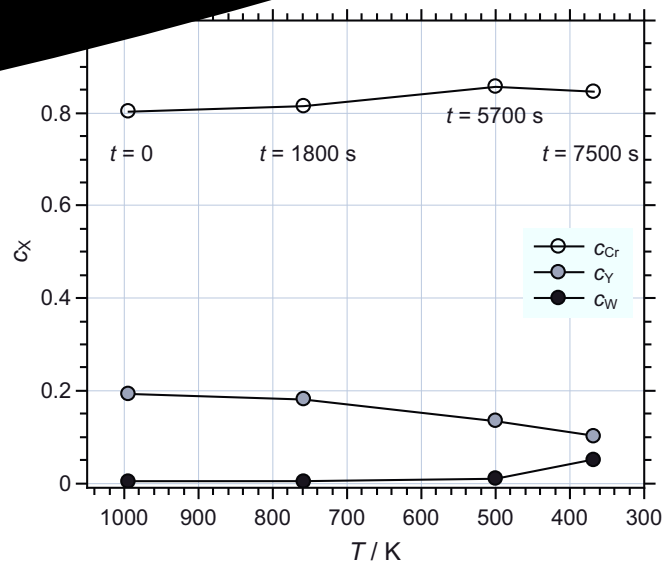

Fig. 6. Fractional surface concentrations, c_X, measured for various temperatures during cooling of the sample. The measurements proceed from left to right. Note that the temperature scale, T, is inverted. The times when each spectrum has been measured are indicated in the figure.

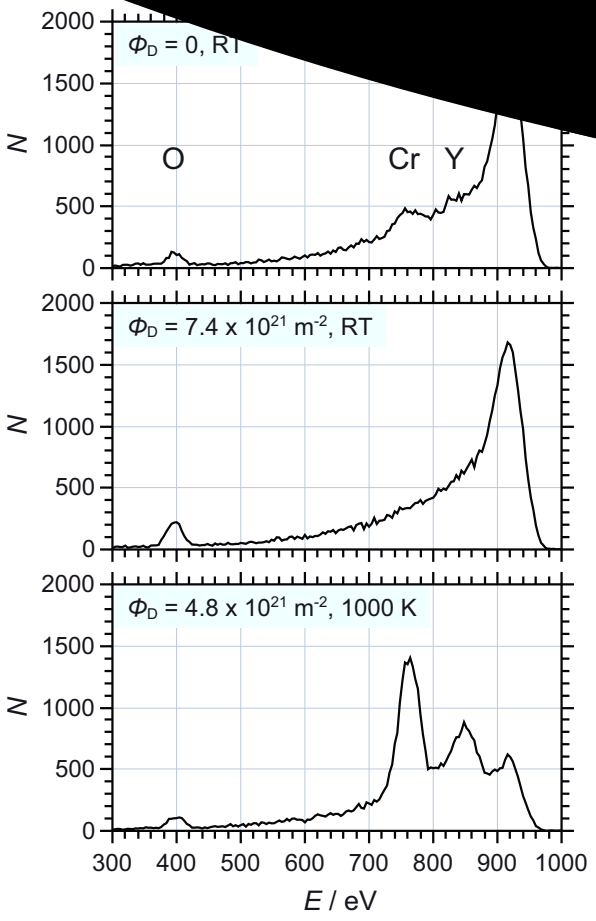

Fig. 7. LEIS spectra showing the preferential sputtering of the lighter alloy constituents. The labels indicate the species which cause the respective scattering peaks. The spectrum after sputter cleaning with Kr is plotted at the top. The plot in the middle shows the spectrum after D sputtering with a fluence of $7.4 \times 10^{21}\,\mathrm{m}^{-2}$ at RT. The plot at the bottom displays the spectrum after a D sputter fluence of $4.8 \times 10^{21}\,\mathrm{m}^{-2}$ at a sample temperature of 1000 K.

for taking a LEIS spectrum is minimised by (i) reducing the scanned energy range to the Cr, Y, and W peaks (neglecting the small O peak) and (ii) shortening the counting time per energy channel to 4000 ms. Both measures reduce the total time for recording a LEIS spectrum to less than 5 min. With a probing ion beam flux $J = 1 \times 10^{16}\,\mathrm{m}^{-2}\mathrm{s}^{-1}$ the maximum Cr sputtering by 1 keV He^+ ions is less than 0.06 monolayers per measurement. During the waiting time between measurements, when the sample temperature is reduced and stabilises at a lower value, the probing ion beam is blanked by increasing the electric potential of the einzel lens in front of the sample. Four measurements are recorded and the respective surface concentrations of Cr, Y, and W are shown in Fig. 6. The temporal order of the measurement is from left to right, i.e. the measurement at the highest temperature is the first one and the measurement at the lowest temperature is the last one in this series. In the figure the times at which the spectra are measured (with respect to the first measurement labelled as $t = 0$) are indicated. When going from a higher to a lower temperature the rates of temperature decay are due to radiation losses only and are rather low, no auxiliary sample cooling is applied. From the time trace of sample temperature versus time one can derive that at the highest temperature the decay rate is less than $0.7\,\mathrm{Ks}^{-1}$, and at the lowest temperature the decay rate is smaller than $0.1\,\mathrm{Ks}^{-1}$. The Cr surface concentration stays fairly constant, whereas the Y surface density decays to about half. The W concentration stays almost zero with the exception of the last measurement which shows a slight increase. The measurement shows that after cool-down of the sample the segregated Cr layer remains on the surface. The small increase of the W surface density visible when the sample temperature falls below 400 K is likely due to the residual sputtering from the LEIS ion beam which preferentially removes Cr and Y atoms from the surface which are not replenished due to the small segregation at low temperature. Within the time of the measurement (>2 h) no de-segregation is visible. This behaviour could result in a chromium oxide layer which might explain the enhanced deuterium retention found in W-10Cr-0.5Y samples which were outgassed at even higher temperatures prior to a study of the hydrogen isotope retention [22].

The preferential sputtering of the WCrY alloy is investigated with impact of 250 eV deuterons. At this energy there is considerable sputtering of Cr, and almost no erosion of W. After preparing the sample in the usual way by Kr sputtering an initial LEIS spectrum is measured. The first preferential sputtering cycle is done at RT with a D fluence of $7.4 \times 10^{21}\,\mathrm{m}^{-2}$. The corresponding LEIS spectra are displayed in Fig. 7. The initial spectrum without D sputtering (top) is similar to the spectrum shown in Fig. 2. After D bombardment (middle) the spectrum exhibits no visible peaks from scattering on Cr or Y. The slight increase of the O peak at 400 eV originates from residual impurities in the D_2 gas which could not be completely removed by the liquid nitrogen trap[3]. The same preferential sputtering investigation is repeated with the sample at a temperature of 1000 K (bottom) using a D fluence of $4.8 \times 10^{21}\,\mathrm{m}^{-2}$. The strong segregation of Cr and Y at this sample temperature prevents the complete removal of Cr and Y from the surface and does not result in a full W coverage as it is observed at RT. Under continuous sputter erosion the lighter segregating alloy constituents Cr and Y are constantly eroded, but at the same time the surface concentrations reach an equilibrium due to the flux of segregating atoms towards the surface. This can be quantified in the following way: The flux of sputtering D atoms with impact energy E onto the surface is J_D. When e.g. Cr covers a surface fraction c_{Cr} and the sputter yield is denoted by $Y_{Cr}(E)$, the flux of eroded Cr atoms is

$$J_{Cr}(T) = c_{Cr}(T, J_D) \times Y_{Cr}(E) \times J_D. \quad (5)$$

[3] The gas can contains up to 50ppm O_2 which, if not reduced by the LN_2 trap, would contribute by 0.1% to the Cr sputtering and about 10% to the W sputtering. However, this would reduce the effect of preferential sputtering what is obviously not observed in the measurement.

$m^{-2}s^{-1}$, $c_{Cr} = 0.55$ (this value of surface coverage corresponds to the 1000 K measurement, dashed line in Fig. 2), and the sputter yield at an energy of 250 eV $Y_{Cr} = 0.04$, the flux of eroded Cr atoms is $2 \times 10^{16}\,m^{-2}s^{-1}$. Note that the sputtered Cr flux in Eq. (5) in the equilibrium state ($dc/dt = 0$) is equal to the flux of Cr atoms which flows from the bulk to the surface due to thermal segregation. This flux depends only on the temperature and on the equilibrium surface coverage and is not specific to the used ion beam setup. However, although Eq. (5) looks rather simple, the surface coverage $c_{Cr}(T, J_D)$ which develops for specific irradiation conditions is non-linear.

It seems still possible to make a rough estimate for the behaviour of a WCrY wall cladding in a future fusion reactor. Using a typical D flux of $1 \times 10^{20}\,m^{-2}s^{-1}$ onto the first wall (Fig. 4 in [23]) and an assumed impact energy of 50 eV, the sputter yield for (elemental) Cr is 1×10^{-4} [24]. The product $Y \times J$ equals $1 \times 10^{16}\,m^{-2}s^{-1}$ which is even lower than (but not very different to) the value obtained in the present ion beam setup. Assuming a resultant Cr surface fraction of e.g. 0.5, which can always be complied at a certain temperature (above 700 K where sufficient segregation occurs), the sputtered Cr flux will be $5 \times 10^{15}\,m^{-2}s^{-1}$, i.e. the flux is of the same order as in the present experiment. The WCrY first wall cladding in a fusion reactor will be rather thin in order not to weaken the tritium breeding ratio too much. Taking a thickness of 2 mm, the area density of Cr atoms will be $4 \times 10^{25}\,m^{-2}$. This number has to be compared to the loss rate of segregated Cr atoms due to sputter erosion which is much smaller and would lead to a reduction of only 0.4% of the Cr atoms per operational year. Re-deposition of sputtered Cr due to the large magnetic field in a fusion device might lead to a further reduction of the loss rate. Even eroding D fluxes larger by one order of magnitude might not be critical at all.

4. Summary and conclusion

The elemental surface composition of self-passivating WCrY samples has been analysed with LEIS at various temperatures up to 1000 K. Strong Cr and Y segregation on the surface occurs above 700 K and W atoms in the topmost surface layer are not detectable at the highest temperature but are still present in the layers beneath the topmost surface layer. Below 700 K a much weaker surface density increase of Cr and Y is observed which might not necessarily be attributed to segregation but could result from the recovery of the equilibrium surface concentrations after the sputter cleaning of the sample. According to the W-Cr phase diagram (NB: a W-Cr-Y phase diagram is not yet available) the alloy with 31% Cr at a temperature of 1000 K is located in the miscibility gap which consists of a mixture of Cr-rich and W-rich solid solutions. The observed segregation can be attributed to grain boundary segregation of these phases. The segregation measurements at the various temperatures are analysed with a Langmuir-McLean relation and yield segregation enthalpies of 0.7 eV for Cr and 0.3 eV for Y in the temperature range above 700 K.

D_2^+ sputtering with 250 eV per deuteron results in preferential sputtering and almost complete Cr depletion from the surface at RT. At an increased sample temperature of 800 K or 1000 K the D sputtering does not completely remove the Cr atoms from the surface. Instead, the strong thermal segregation still yields an increase of the Cr surface concentration. The equilibrium between sputter erosion and segregation allows to determine the flux of Cr atoms towards the surface which are eroded and lost from the bulk.

Although the Cr segregation prevents the build up of a complete W layer, no serious issue which might question the application of the WCrY alloy for the intended purpose has emerged by this finding. The enhancement of Cr erosion is rather weak and and extrapolation for the conditions in a fusion reactor yields Cr losses less than 1% per operational year. In case of a loss-of-coolant accident the Cr enrichment on the surface might even turn out to be beneficial because it accelerates the formation of the protecting chromium oxide layer.

CRediT authorship con

Hans Rudolf Koslowski: Conceptualiza analysis, Software, Visualization, Writing - origina **Schmitz:** Conceptualization, Investigation, Formal analysis, Writing review & editing. **Christian Linsmeier:** Writing - review & editing.

Declaration of Competing Interest

The authors declare that they have no known competing financial interests or personal relationships that could have appeared to influence the work reported in this paper.

Acknowledgements

We thank Mr. Albert Hiller and Mr. Roland Bär for technical assistance and maintenance of the apparatus, and Mrs. Beatrix Göths for polishing the WCrY sample. Helpful discussion on the role of the chromium oxide layer for hydrogen retention with Dr. Hans Maier (IPP Garching) is very much acknowledged. This work has been carried out within the framework of the EUROfusion Consortium and has received funding from the Euratom research and training programme 2014–2018 and 2019–2020 under grant agreement No 633053. The views and opinions expressed herein do not necessarily reflect those of the European Commission.

References

[1] H. Bolt, V. Barabash, G. Federici, et al., Plasma facing and high heat flux materials - needs for ITER and beyond, J. Nucl. Mater. 307–311 (2002) 43–52, https://doi.org/10.1016/S0022-3115(02)01175-3.
[2] R. Neu, J. Riesch, J.W. Coenen, et al., Advanced tungsten materials for plasma-facing components of DEMO and fusion power plants, Fusion Eng. Des. 109–111 (2016) 1046–1052, https://doi.org/10.1016/j.fusengdes.2016.01.027.
[3] D. Maisonnier, D. Campbell, I. Cook, et al., Power plant conceptual studies in Europe, Nucl. Fusion 47 (2007) 1524–1532, https://doi.org/10.1088/0029-5515/47/11/014.
[4] F. Koch, J. Brinkmann, S. Lindig, et al., Oxidation behaviour of silicon-free tungsten alloys for use as the first wall material, Phys. Scr. T145 (2011) 14019, https://doi.org/10.1088/0031-8949/2011/T145/014019.
[5] A. Litnovsky, T. Wegener, F. Klein, et al., New oxidation-resistant tungsten alloys for use in the nuclear fusion reactors, Phys. Scr. T170 (2017) 14012, https://doi.org/10.1088/1402-4896/aa81f5.
[6] J. Schmitz, A. Litnovsky, F. Klein, et al., WCrY smart alloys as advanced plasma-facing materials – Exposure to steady-state pure deuterium plasmas in PSI-2, Nucl. Mater. Energy 15 (2018) 220–225, https://doi.org/10.1016/j.nme.2018.05.002.
[7] H.H. Brongersma, M. Draxler, M. de Ridder, P. Bauer, Surface composition analysis by low-energy ion scattering, Surf. Sci. Rep. 62 (2007) 63–109, https://doi.org/10.1016/j.surfrep.2006.12.002.
[8] D.P. Smith, Analysis of Surface Composition with Low-Energy Backscattered Ions, Surf. Sci. 25 (1971) 171–191, https://doi.org/10.1016/0039-6028(71)90214-7.
[9] H. Niehus, W. Heiland, E. Taglauer, Low-energy ion scattering at surfaces, Surf. Sci. Rep. 17 (1993) 213–303, https://doi.org/10.1016/0167-5729(93)90024-J.
[10] H.R. Koslowski, S.R. Bhattacharyya, P. Hansen, et al., Temperature-dependent in-situ LEIS measurement of W surface enrichment by 250 eV D sputtering of EUROFER, Nucl. Mater. Energy 16 (2018) 181–190, https://doi.org/10.1016/j.nme.2018.07.001.
[11] W.L. Patterson, G.A. Shirn, The Sputtering of Nickel-Chromium Alloys, J. Vac. Sci. Technol. 4 (1967) 343–346, https://doi.org/10.1116/1.1492560.
[12] Y. Yamamura, H. Tawara, Energy Dependence of Ion-Induced Sputtering Yields from Monoatomic Solids at Normal Incidence, At. Data Nucl. Data Tables 62 (1996) 149–253, https://doi.org/10.1006/adnd.1996.0005.
[13] E. Taglauer, W. Heiland, Surface Analysis with Low Energy Ion Scattering, Appl. Phys. 9 (1976) 261–275, https://doi.org/10.1007/BF00900452.
[14] D. Rapp, P. Englander-Golden, D.D. Briglia, Cross Sections for Dissociative Ionization of Molecules by Electron Impact, J. Chem. Phys. 42 (1965) 4081–4085, https://doi.org/10.1063/1.1695897.
[15] K. Sugiyama, K. Schmid, W. Jacob, Sputtering of iron, chromium and tungsten by energetic deuterium ion bombardment, Nucl. Mater. Energy 8 (2016) 1–7, https://doi.org/10.1016/j.nme.2016.05.016.
[16] A. Litnovsky, F. Klein, J. Schmitz, et al., Smart first wall materials for intrinsic safety of a fusion power plant, Fusion Eng. Des. 136 (2018) 878–882, https://doi.org/10.1016/j.fusengdes.2018.04.028.
[17] G.C. Nelson, Summary Abstract: Semiempirical modeling of the background in low energy ion scattering spectra, J. Vac. Sci. Technol. A 4 (1986) 1567–1569, https://doi.org/10.1116/1.573508.
[18] R. Beikler, E. Taglauer, Surface segregation at the binary alloy CuAu (100) studied

scattering, Surf. Sci. 643 (2015) 138–141, https://doi.org/10.
j.susc.2015.08.030 0039-6028.
[19] M.P. Seah, Grain boundary segregation, J. Phys. F: Metal Phys. 10 (1980) 1043–1064, https://doi.org/10.1088/0305-4608/10/6/006.
[20] G. Tauber, H.J. Grabke, Grain Boundary Segregation of Sulfur, Nitrogen, and Carbon in α-Iron, Ber. Bunsenges. Phys. Chem. 82 (1978) 298–302, https://doi.org/10.1002/bbpc.197800042.
[21] S.V.N. Naidu, A.M. Sriramamurthy, P. Rama Rao, The Cr-W (Chromium-Tungsten) System, Bull. Alloy Phase Diagr. 5 (1984) 289–292, https://doi.org/10.1007/BF02868555.
[22] H. Maier, T. Schwarz-Selinger, R.
materials for fusion applications, Nucl.
doi.org/10.1016/j.nme.2018.12.032.
[23] R. Behrisch, G. Federici, A. Kukushkin, D. Reiter, Material erosion
of future fusion devices, J. Nucl. Mater. 313–316 (2003) 388–392, https://
10.1016/S0022-3115(02)01580-5.
[24] W. Eckstein, Sputtering Yields, Top. Appl. Phys. 110 (2007) 33–187, https://doi.org/10.1007/978-3-540-44502-9_3.